

SCIENTIFIC REPORTS



OPEN

Functional analysis of *CYP6ER1*, a P450 gene associated with imidacloprid resistance in *Nilaparvata lugens*

Received: 24 June 2016
Accepted: 22 September 2016
Published: 10 October 2016

Rui Pang^{1,*}, Meng Chen^{1,*}, Zhikun Liang¹, Xiangzhao Yue¹, Hu Ge² & Wenqing Zhang¹

The cytochrome P450 *CYP6ER1* has been reported to play an important role in imidacloprid resistance of the brown planthopper (BPH), *Nilaparvata lugens*, and is overexpressed in most resistant populations. In the present study, we confirmed that *CYP6ER1* expression can be induced by certain levels of imidacloprid. Developmental expression analysis revealed that *CYP6ER1* was expressed highly in the adult stage, and tissue distribution analysis showed that *CYP6ER1* was expressed mainly in the fat body and midgut. RNA interference (RNAi) of *CYP6ER1* and transgenic expression of *CYP6ER1* in *Drosophila melanogaster* both suggested that the expression of *CYP6ER1* is sufficient to confer imidacloprid resistance. Furthermore, we analyzed the interaction of imidacloprid and *CYP6ER1* monooxygenase by using dynamic simulations and molecular docking. We found that Nitrogen atoms in the heterocycle of the imidacloprid molecule may bind to iron atoms in the center of the homology model of *CYP6ER1* via 4,5-dihydro-1H-imidazole. This finding contributes to a better understanding of how *CYP6ER1* takes part in the insecticide metabolism.

The brown planthopper (BPH), *Nilaparvata lugens* is one of the monophagous rice insect pests, whose outbreaks in can cause great losses in rice producing regions. To protect rice crops from serious damage by *N. lugens*, the widespread application of insecticide has been implemented by many farmers¹. However, after over 30 years of insecticide use to control rice planthopper infestations in China and other areas of Asia, it has become apparent that the chronic application of any kind of insecticide can lead to the development of resistance, and this resistance has emerged as a major problem in *N. lugens* control². Within field populations of *N. lugens* resistance to major insecticide classes, such as organochlorines^{3,4}, organophosphates^{5,6}, carbamates³, pyrethroids⁷, buprofezin⁸, neonicotinoids⁹, fipronil¹⁰, and pymetrozine¹¹, has emerged.

Insecticide resistance involves a variety of mechanisms, such as reduction of penetration rate, enhancement of metabolic detoxification, accelerated excretion of insecticides from the organism and target site insensitivity. Enhancement of P450 monooxygenase enzymatic activity related to insecticides resistance, especially to neonicotinoid insecticides, is a typical case of enhancement of metabolic detoxification¹². *In vivo* suppression or decrease in resistance by application of P450 inhibitors such as the synergist piperonyl butoxide is often used as a diagnostic for P450 involvement¹³. In many cases, the over-expression or up-regulation of P450, can increase pests' ability to resist to insecticide. An example of this is, *CYP6G1* overexpression in *Drosophila* and the associated resistance to DDT¹⁴. *CYP6D1* causes resistance to pyrethroid in house flies¹⁵, and *CYP4E3* expression results in permethrin insecticide tolerance in *Drosophila*¹⁶. In BPH, a single P450 gene, *CYP6ER1*, is thought to play an important role in imidacloprid resistance^{17–19}. The overexpression of *CYP6ER1* has been found in most resistant strains and the level of expression observed in the different BPH strains was significantly correlated with the resistance phenotype¹⁹. In addition, a previous study indicated *CYP6ER1* metabolized imidacloprid less efficiently compared to *CYP6AY1* but it could be upregulated by imidacloprid²⁰.

However, it is impossible to predict catalytic activity of P450s based on sequence alignments in order to give deeper insight into their mechanisms of insecticides metabolism²¹. Protein modeling is a method to obtain

¹State Key Laboratory of Biocontrol, School of Life Sciences, Sun Yat-sen University, Guangzhou, 510006 China.

²School of Pharmaceutical Science, Sun Yat-sen University, Guangzhou, 510006 China. *These authors contributed equally to this work. Correspondence and requests for materials should be addressed to W.Z. (email: lsszwq@mail.sysu.edu.cn)

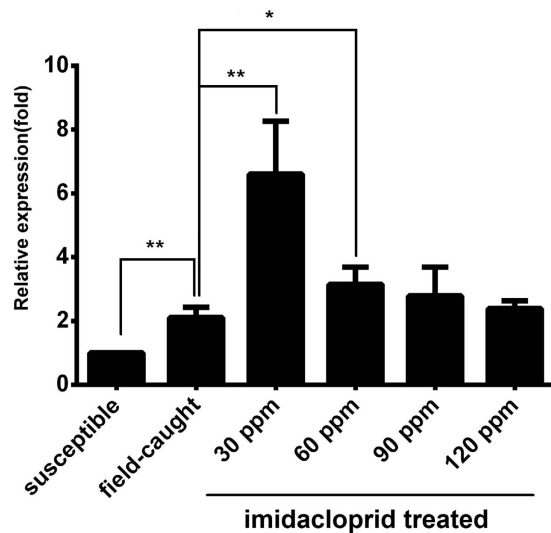


Figure 1. *CYP6ER1* expression patterns in response to insecticide exposure. Quantitative real-time PCR measurement of the fold change in the expression of *CYP6ER1* in the field-caught strain compared with the susceptible strain, while the field-caught strain treated with 4 different doses of imidacloprid (30ppm,60ppm,90ppm and 120ppm, respectively) compared with the field-caught strain without imidacloprid. β -actin was used as an internal reference gene and the mRNA expression level of *CYP6ER1* in the susceptible strains was designated as one. The data represent the mean + SEM (n = 30). * $P < 0.05$ level (t -test) and ** $P < 0.01$ level (t -test).

structural data when experimental techniques fail. Many proteins are too large for NMR analysis and cannot be crystallized for X-ray diffraction²², resulting in a lack of elucidate crystal structures for P450s and their substrate complexes. In these cases, homology modeling gives an insight into understanding the complexity of insecticide resistance mediated by P450 genes^{23,24}. By comparing homologous candidates, a number of candidates searched in the database can, to a certain extent, allow researchers to predict and visualize specific molecular structures and interactions, which are difficult to prove using traditional biological experiments. Jones utilized homology modeling based on a template of the X-ray structure of the phylogenetically related human CYP3A4, to simulate the interaction between *D. melanogaster* CYP6G1 and DDT and neonicotinoids, and indicated roles for CYP6G1, CYP12D1 and CYP6A2 in flies overexpressing P450 enzymes with broad substrate specificities in chemical metabolism²⁵. Karunker found interactions of imidacloprid with the biotype Q variant of the CYP6CM1 enzyme might involve key amino acids such as Phe-130 and Phe-226 in the enzyme active site with the lowest energy, and they predicted a putative hydroxylation site²⁶. Unfortunately, while the application of homology modeling is now widely spread in the medical sciences, it has been used in only a limited capacity for the determination of insecticide metabolism mechanisms in pest control.

In this study, we determined, using RNAi and transgenic expression in *Drosophila*, that the expression of P450 *CYP6ER1* is sufficient to confer imidacloprid resistance. Additionally, we utilized molecular modeling in order to predict the catalytic site geometrics and identify the key residues responsible for imidacloprid binding with *CYP6ER1*. These experiments contribute to clarifying the enzyme responsible for metabolizing imidacloprid and causing the resistance phenotype.

Results

***CYP6ER1* expression patterns in response to insecticide exposure.** In order to confirm the expression pattern of *CYP6ER1* in insecticide resistant BPH strains, one-day-old female adults of a field-caught strain from Guangxi and a susceptible contrasted strain from Zhejiang were selected and the field-caught strain was further treated with 4 different doses of imidachloprid. We found that the mRNA level of *CYP6ER1* in the field-caught strain was 2.1-fold higher than that observed for the susceptible strain, and the mRNA expression level in the samples treated with 30 ppm and 60 ppm imidachloprid was significantly higher than that observed for the untreated field-caught strain. However, there was no significant difference between the untreated field-caught strain and samples treated with 90 ppm or 120 ppm imidachloprid (Fig. 1). These results suggested that the up-regulation of *CYP6ER1* can be triggered by imidachloprid, and it can reach at maximum within certain dosages of imidachloprid.

Developmental expression and tissue distribution of *CYP6ER1*. Quantitative Real-time PCR (qRT-PCR) was used to detect the expression patterns of *CYP6ER1* during *N. lugens* from the first instar nymphs to the 13th day adulthood. The mRNA levels developed a stable trend of low expression before 5th instar, but increased significantly from adult day 1 to a relatively high level between adult day 9 and day 13 (Fig. 2A). We also sampled different tissues from 1-day-old female adults to investigate their mRNA levels of *CYP6ER1*, and it was expressed highly in the fat body and midgut, expressed at a relatively lower level in the ovaries, Malpighian tubule

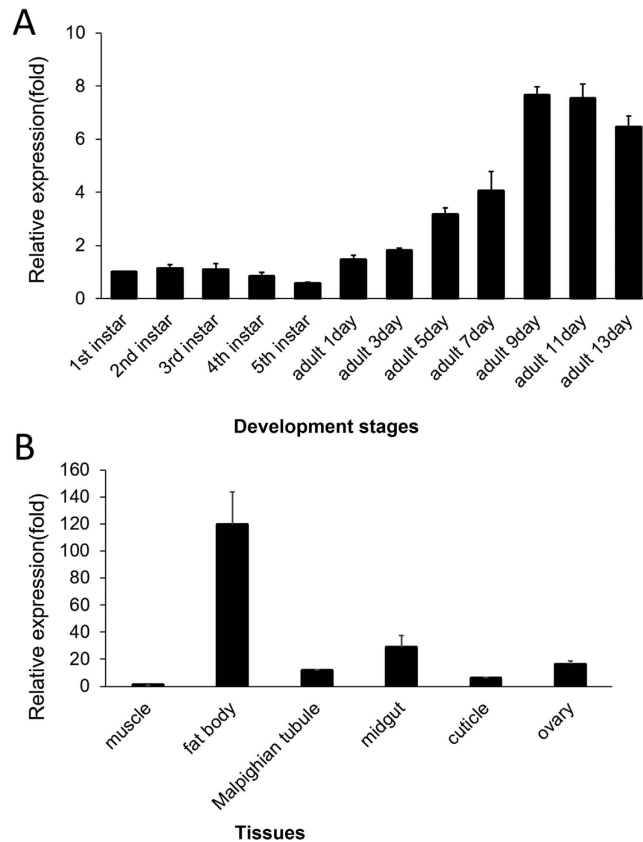


Figure 2. Developmental expression and tissue distribution of CYP6ER1. (A) Developmental expression of CYP6ER1 mRNA by qRT-PCR. Nymphs 1–5: the 1st instar nymphs to the 5th instar nymphs; Adults odd day of 1–13 days: female adults from the odd day of 1 to 13 days. The mRNA levels of CYP6ER1 were relative to the β -actin mRNA level and the mRNA expression level in 1st instar are designated as one. The data represent the mean + SEM (n = 30). (B) Tissue distribution of CYP6ER1. Fat body, Ovary, Midgut, Cuticle, Malpighian tubule and muscle. The mRNA levels of CYP6ER1 were relative to the β -actin mRNA level and the mRNA expression level in muscle is designated as one. The data represent the mean + SEM (n = 3).

and cuticle, and not expressed in the muscle (Fig. 2B). The high levels of expression in the essential metabolic organs correspond to the physiological role of CYP6ER1 in imidacloprid resistance.

RNA interference of CYP6ER1. To evaluate the contributions of CYP6ER1 in imidacloprid resistance *in vivo*, we designed dsRNA to silence CYP6ER1 in female adult from the Guangxi strain. The mRNA expression of CYP6ER1 decreased within 48 hours after injecting three doses (50 ng, 100 ng and 200 ng) of dsCYP6ER1, but there was no significant difference between the three doses of dsRNA (Fig. 3A). We chose 50 ng imidacloprid treatment for 48 hours to test BPH mortality after RNAi (Fig. 3B). The mortality of the dsCYP6ER1 sample was 40.00% and 34.42% higher than those of the ddH₂O and dsGFP samples, respectively. This suggests that the expression of CYP6ER1 should be of great importance to imidacloprid resistance in BPH.

Transgenic expression of the potential resistance genes CYP6ER1 in *D. melanogaster*. To identify whether the expression of CYP6ER1 is sufficient to confer imidacloprid resistance, we used a transgenic approach utilizing the GAL4/UAS system of *D. melanogaster*. CYP6ER1 was inserted into the vector pUAST and embryonic microinjections were performed on *D. melanogaster* w¹¹¹⁸ to generate the transgenic germline carrying a UAS-CYP6ER1 transgene. The flies subsequently were crossed to the Act5C-GAL4 line. The mRNA levels of CYP6ER1 were determined in the progeny (1–3 days-old adults) by RT-PCR, confirming the expression of the transgene in the Act5C >CYP6ER1 line (progeny expressing the CYP6ER1) (Fig. 4A). In comparison, the CYP6ER1 mRNA was not detected in another two control *D. melanogaster* lines (UAS-CYP6ER1 and Act5C-GAL4, progeny not expressing the CYP6ER1).

Bioassays showed that Act5C >CYP6ER1 line was resistant to imidacloprid at a treated dose of 30 μ g/ml imidacloprid, with significant higher survival rate (86.42%, $p < 1e-10$ Chi-squared Test) than the control lines (4.23% and 11.15% respectively) (Fig. 4B). These results suggest that the expression of CYP6ER1 confers imidacloprid resistance.

Homology modelling of CYP6ER1. Structure based sequence alignment was used to compare the key residues previously predicted to be responsible for imidacloprid binding and metabolism, such as CYP6CMA1,

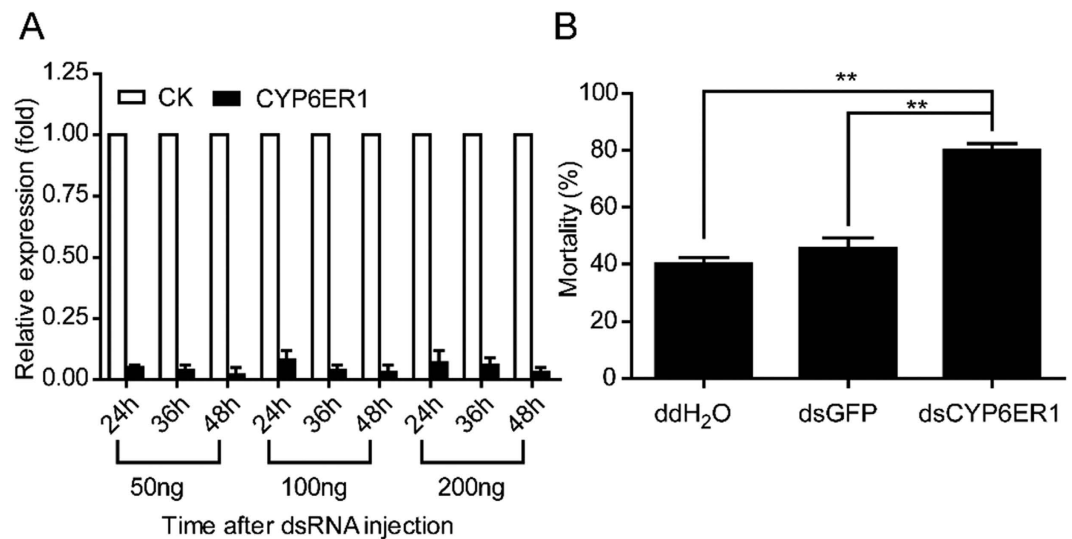


Figure 3. Detection of the mRNA level and mortality after RNA interference (RNAi). (A) The *CYP6ER1* mRNA expression level after injecting three doses (50 ng, 100 ng and 200 ng) of ds*CYP6ER1* at three time points. The mRNA expression level of *CYP6ER1* in ds*GFP* ground and ds*CYP6ER1* group were relative to β -actin mRNA level and the mRNA expression level of *CYP6ER1* in ds*GFP* group was designated as one. (B) Effects on the mortality rate after injection of water or ds*GFP* or ds*CYP6ER1* and followed by application of imidacloprid (50 ng/ml). Double asterisks indicate significant differences in the mRNA relative expression level between the treatment and control groups ($P < 0.01$, *t*-test). The data represent the mean \pm SEM ($n = 3$), $**P < 0.01$ level (*t*-test).

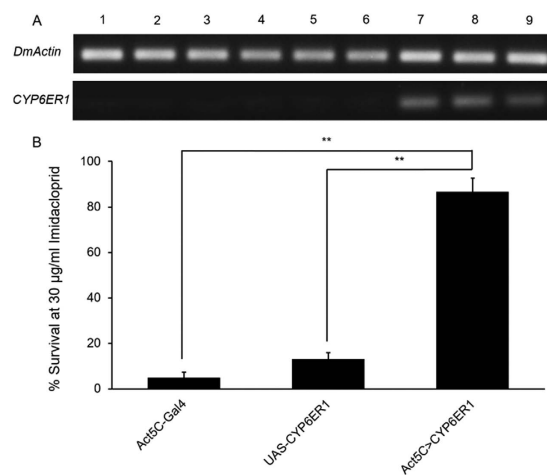


Figure 4. Transgenic expression of *CYP6ER1* in *D. melanogaster* and its effect on imidacloprid resistance. (A) The expressions of *CYP6ER1* were confirmed by RT-PCR in two control lines and transgenic line. 1, 2, 3, three biological replicates of Act5C-GAL4, flies with genetic background correspond to Act5C-GAL4; 4, 5, 6, three biological replicates of UAS-*CYP6ER1*, flies not expressing the *CYP6ER1*; 7, 8, 9, three biological replicates of Act5C>*CYP6ER1*, transgenic flies expressing the *CYP6ER1*. (B) The comparison between survival rates of two control lines and transgenic line exposed to 30 μ g/ml imidacloprid. The data shown are the mean \pm SEM ($n = 3$). $**P < 0.01$ (Chi-squared Test).

CYP3A4, and CYP6G1 (Fig. 5; Table 1). CYP6ER1 had a high similarity and shared several functionally identical amino acids, suggesting that CYP6ER1 may have the same functional domain as other imidacloprid metabolism proteins. The prediction of the substrate recognition site (SRS) secondary structure elements and key residues were cited in the research of CYP6CM1²⁶. A BLAST search with the default parameters for CYP6ER1 in the PDB_nr95 database identified the homologous protein, CYP3A4 (PDB code: 3NXU), with an intermediate sequence identity of 31%, which was then used to construct the CYP6ER1 structure.

A total of 20 models were generated. Among these 20 models, 6ER1.M0011 had the smallest value of PDF (probability density function) Total Energy and PDF Physical Energy, and relatively low DOPE Score (Table S3), by using Cut overhangs, refine loops and use of DOPE method as parameters. This indicated that 6ER1.M0011

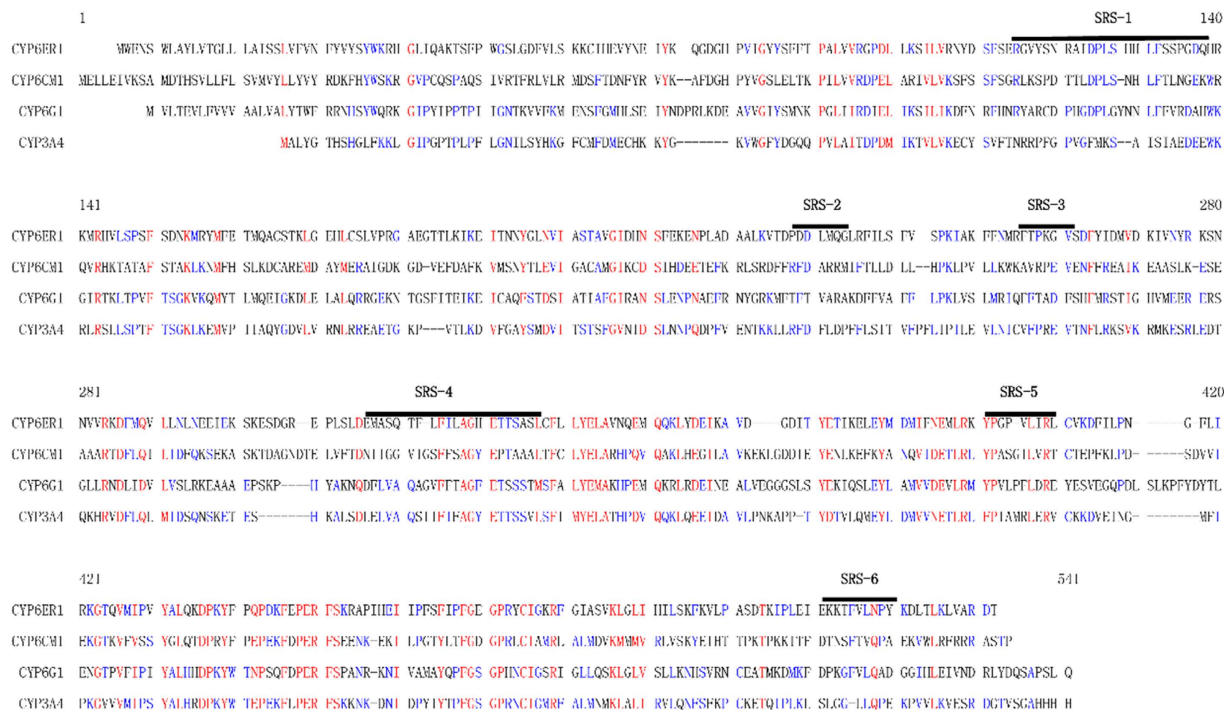


Figure 5. Sequence alignment of *CYP6CM1vQ*, *CYP3A4*, *CYP6ER1* and *CYP6G1*. Sequences are colored red for identity and colored blue for similarity. The substrate recognition site (SRS) regions are represented by a black line.

<i>CYP6ER1</i>	<i>CYP6CM1</i>	<i>CYP3A4</i>	<i>CYP6G1</i>	SRS location	Secondary structure
124Phe	130Phe	98Ser	124Phe	SRS-1	Loop between helices B and C
288Asp	224PHe	190Leu	218Phe	SRS-2	Loop between helices F and F'
289Pro	225Arg	191Arg	219Thr	SRS-2	Loop between helices F and F'
290Asp	226Phe	192Phe	220Phe	SRS-2	Loop between helices F and F'
246Phe	251Ala	219Val	245Phe	SRS-3	Loop between helices G' and G
247Thr	252Val	220Phe	246Phe	SRS-3	Loop between helices G' and G
312Leu	321Ser	283Phe	311Thr	SRS-4	Helix I (O ₂ binding motif)
313Ala	322Ala	284Ala	312Ala	SRS-4	Helix I (O ₂ binding motif)
314Gly	323Gly	285Gly	313Gly	SRS-4	Helix I (O ₂ binding motif)
317Thr	326Pro	288Thr	316Thr	SRS-4	Helix I (O ₂ binding motif)
374Gly	387Ala	348Ile	377Val	SRS-5	Loop between helix K and b-strand
375Pro	388Ser	349Ala	378Leu	SRS-5	Loop between helix K and b-strand
376Val	389Gly	350Met	379Pro	SRS-5	Loop between helix K and b-strand
487Thr	501Ser	460Gly	497Gly	SRS-6	C-terminal loop
488Phe	502Phe	461Gly	498Phe	SRS-6	C-terminal loop
489Val	503Thr	462Leu	499Val	SRS-6	C-terminal loop

Table 1. Alignment of the analogous imidacloprid binding residues in four imidacloprid metabolizing enzymes: *CYP6ER1*, *CYP6CM1*, *CYP3A4*, *CYP6G1*. Analyses were based on structure sequence alignment between the *CYP6CM1* model and the *CYP3A4* crystallographic structure together with sequence alignment to *CYP6G1*. Some of the residues that contribute to the stabilization of imidacloprid in the active site are also important in the stabilization of the heme and oxygen molecules.

was the most suitable model among the 20 counterparts, and could be utilized to simulate the molecular docking. 6ER1.M0011 was then analyzed by Ramachandran and most of these residues were located in the most favored region, with 11 out of 470 residues in the disallowed region, suggesting it was a relatively good quality model but needed further regulation and optimization.

The binding mode of imidacloprid to the *CYP6ER1* active site. During our analysis, we found ritonavir as specific inhibitor of *CYP3A4* in human, which suggested that its docking method may be similar to

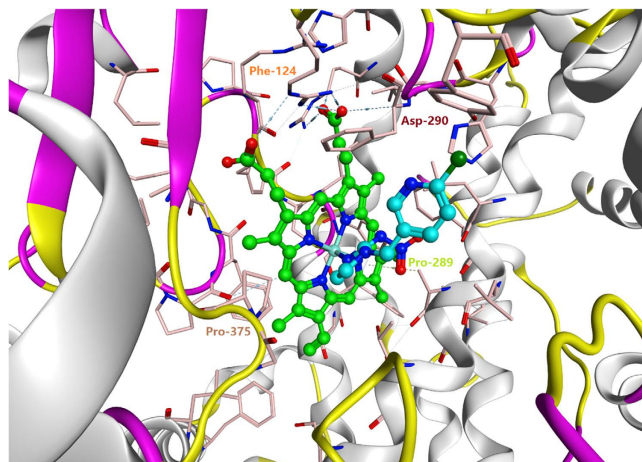


Figure 6. Overview of P450-HEME-IM4 complex and its binding pocket. The one conformation of MD-based optimized structure. Imidacloprid is indicated with light blue carbon atoms and the HEME is shown with grass green atoms. Predicted binding residues within 4 Å of imidacloprid are shown in pink. Phe-124 and Asp-290 anchor imidacloprid by aromatic interactions, and generate significant part of the contact surface area. Imidacloprid may be further stabilized by hydrogen bonded with Pro-375 and Pro-289.

CYP6ER1. Imidachloprid and ritonavir both have a similar heterocycle (Fig. S1A,B) and ESP charge distribution (Fig. S1C,D). Ritonavir bonds covalently to CYP3A4 via nitrogen atoms, and this mode may be similar to the way imidachloprid bonds to CYP6ER1.

We used the homology model based on CYP6ER1 as the receptor, and the imidachloprid molecule as the ligand. Nitrogen atoms in the heterocycle of the imidachloprid molecule bonded to iron atoms in the center of the homology model via 4,5-dihydro-1H-imidazole. The temperature of CYP6ER1-imidachloprid compound hovered around 300 K, with its deviation below 10 K (Fig. S2), and the total energy, kinetic energy and potential energy started from high energy to a stable relatively low level after about 5 picoseconds (Fig. S3). RMSD of atomic coordination of the protein backbone, HEME and ligand fluctuated up and down in the range between 1.20 Å to 1.50 Å (Fig. S4). The results confirmed the hypothesis of the formation of a CYP6ER1-imidachloprid complex based on its relatively credible stability and balance of its energy and the structure. Finally, the interaction energy of CYP6ER1-imidachloprid complex was calculated at -114.66 kcal/mol, indicating that this may be the ideal model to simulate the P450-HEME-IM4 complex and its binding pocket, and suggested that some amino acids in the center of CYP6ER1 have a role in the molecular docking between CYP6ER1 and imidachloprid (Figs 5 and 6 and Table 1). Most of these residues were predicted to generate the hydrophobic interface of the binding cavity, in which Phe-124 was predicted to anchor imidachloprid by aromatic interaction generating the largest hydrophobic patch in the interface. We predicted that imidachloprid would be further stabilized by hydrogen donors and acceptors that include Pro-375 (SRS-5) and Pro-289 (SRS-2), which can interact with imidachloprid's imine moiety and Leu-312(SRS-4).

Discussion

It is generally believed that detoxifying enzymes, referred to as esterase, glutathione S-transferase and P450s, contribute to defending against and catabolizing toxins and insecticides in insects, and that many involve point mutations of target genes for insecticide which increase the copy number of the gene, mRNA level and the diversification of the coding sequence²⁷. In a study of neonicotinoids, total enzyme activities of the candidate metabolic enzymes were measured in *N. lugens*, indicating that the increase of neonicotinoids resistance was due mainly to P450 monooxygenase, instead of mutations of the nicotinic acetylcholine receptors that were considered as possible targets²⁸. Puinean used piperonyl butoxide, an inhibitor specific to P450s, to decrease the level of imidachloprid resistance significantly, which confirmed the important roles of P450s in insecticide resistance²⁹. Similarly, the phenomenon was also reported in aphids³⁰. Additionally, specific P450 genes have been related to neonicotinoids resistance. For instance, *Drosophila CYP6G1* has been proven to confer imidachloprid resistance^{14,31}, and Puinean suggested that *CYP6Y3* can confer neonicotinoids resistance to *Myzus persicae*³².

The P450 CYP6ER1 has been associated with imidachloprid resistance in *N. lugens*¹⁹. Here, we found that the mRNA level of *CYP6ER1* was significantly higher in the field-caught resistant strains than in the susceptible strains, which generally coincides with previous references. Susceptibility to imidachloprid increased by 75.61% after RNAi treatment in the experimental population (Fig. 3). Similarly, it has been reported that susceptibility to Deltamethrin in *Locusta migratoria* increased by 92.14% and 72.93% after RNAi knockdown of *CYP409A1* and *CYP409B1*, respectively. Additionally, transgenic expression of *CYP6ER1* in *D. melanogaster* lead to a significant increase of imidachloprid resistance. We therefore conclude that the expression of *CYP6ER1* is sufficient to confer imidachloprid resistance. Of particular note is that fact that, though the expression of *CYP6ER1* in the resistant strain can be induced by imidachloprid treatment, the over-expression of this gene was limited when BPH were treated by a relatively higher dose of imidachloprid. This indicates that the imidachloprid resistance phenotype may

be more complex than just the over-expression of a single gene. Thus, it is necessary to review and optimize the traditional strategy of pest control.

P450 monooxygenase is well known for metabolizing xenobiotics, such as insecticides, to less toxic metabolites^{33,34}. For example, CYP6A1, 6A2, 6A5, and 12A1 all have some manner of cyclodiene epoxidase biochemical activity. Graham and Peterson observed the general topology and tridimensional fold of all cytochromes P450³⁵. Only a few strictly conserved residues, as components of a four-helix (D, E, I and L) bundle, two sets of β -sheets, and a coil, participate to form the center of P450s together with a central heme-group bound to the thiolate of a relatively highly conserved cysteine residue, which give access to the biotransfer of electrons and protons to activate oxygen. On the other hand, the individual substrate specificity of the enzymes lies on the individual residues despite their homologous and similar regions, conferring their unique function in reactions with different insecticides.

Over-expression of *CYP6ER1* was able to confer imidacloprid resistance, and this could be induced by certain doses of imidacloprid itself. Therefore, it is important to explore further the interaction between CYP6ER1 and imidacloprid. Utilizing homology modeling technology, and based on the high degree of homology with CYP3A4 in human, we predicted and visualized the molecular interaction wherein nitrogen atoms in the heterocycle of the imidacloprid molecule bond mainly to iron atoms in the center of the homology model via 4, 5-dihydro-1H-imidazole. CYP6CMAvQ and CYP6G1, two identified P450s which detoxify imidacloprid, were referred to our alignment with CYP6ER1 and CYP3A4^{26,36}, confirming that target sequences and the substrate recognition site (SRS) regions had a high level of similarity²⁶. Alignment of analogous imidacloprid binding residues in these four imidacloprid metabolizing enzymes indicated a number of consistent binding residues among them. To assess the stability and the balance of the CYP6ER1-imidacloprid complex, several parameters in the field of energetic and geometric criteria were calculated and analyzed until we obtained an optimized model to simulate the interaction. After optimization, our homology model proved to be of high quality. Additionally, there were some putative key residues responsible for imidacloprid binding with similarity among the four enzymes, most of which create the hydrophobic interface of the binding cavity, as suggested by the docking analysis. Phe-124 and Asp-290 anchor imidacloprid by aromatic interactions, and create a significant part of the contact surface area between imidacloprid and CYP6ER1. Pro-375 (SRS-5) and Pro-289 (SRS-2) likely generate hydrogen bonds to further stabilize imidacloprid. In these residues interacting with imidacloprid, Ala-313 and Gly-314 are conserved in three other imidacloprid metabolizing enzymes: CYP6CM1, CYP3A4 and CYP6G1. The conservation of these residues and the relative large hydrophobic contact surface area, show that residues play an important role in contributing to these enzymes function of metabolizing imidacloprid. However, we cannot ignore the possibility of other residues constructing the model, despite the lack of apparent homologues among these enzymes, which may develop its own specific function and structure for the enzyme.

Our findings have demonstrated the importance of homology modelling and docking to search the potential catalytic center of an enzyme with its substrate. Our research can also lead a strong foundation for future insecticide design. However, a deeper understanding of the interaction mode of imidacloprid related heterocyclic compounds with P450s is needed in order to guide the rational development of insecticide-related compounds and increasing the accuracy and efficiency of computational based drug construction. In addition, the predicted residues and sites involved in detoxifying imidacloprid require further biochemical validation.

Material and Methods

Insect strains. The field-caught strains were collected from Nanning, Guangxi, China in 2012, and provided by Institute of Plant Protection, Guangxi Academy of Agricultural Sciences. The susceptible strains were obtained from Zhejiang Academy of Agricultural Sciences in 2012 and reared on rice plants without insecticide treatment. The resistance ratios for imidacloprid of the field-caught strain (LC_{50} 249.13 mg/L) to the susceptible strain (LC_{50} 0.22 mg/L) was 1132-fold.

Insecticide exposure. Imidacloprid (96.04%) was purchased from Tianyuan Biochemical Co. Ltd (Guangxi, China). We use the rice stem dipping method for insecticide exposure to BPH as described³⁷. Different doses of imidacloprid were diluted with acetone to a series of concentrations, and then 1% Tween 80 was added. Rice stems rooted in culture cups were dipped in insecticide solutions for 30 s. Once the stems were dry, one-day-old long-winged female adults were put into each culture cup and fed on these treated rice. Each treatment was performed in triplicate.

Total RNA extraction. Total RNA was extracted from BPH by using a Total RNA extract kit (Omega). Genomic DNA was digested with DNase I (Takara Bio Inc., Kyoto, Japan). The quality and concentration of RNA samples were examined by agarose gel electrophoresis and spectrophotometric analysis. cDNA was synthesized by reverse transcription in 20 μ l reaction volumes containing 1 μ g of total RNA by using PrimeScript reverse transcriptase (Takara). The reaction mixture was stored at -20°C for future use³⁷.

qRT-PCR. Primers were designed for qRT-PCR based on the complete coding sequences of *CYP6ER1* genes as archived in the NCBI database (Table S1). The primers had annealing temperatures of approximately 58°C . Primers corresponding to the housekeeping gene *β -Actin* were used as endogenous controls³⁸. qRT-PCR was performed in a LightCycler480 (Roche, Indianapolis, IN, USA) using a SYBR Premix Ex Taq Kit (Roche) with the following conditions: 95°C for 5 min, 40 cycles of 95°C for 10 s, 58°C for 20 s and 72°C for 20 s. For the final melting curve step, the samples were subjected to 95°C for 5 s, held at 65°C for 1 min and then ramped to 97°C in 5°C increments every 1.5 s. A final cooling step held the samples at 40°C . All qRT-PCR analysis was based on three independent experiments. After three repeat PCR experiments, the gene expression level was calculated using the $2^{-\Delta\Delta\text{CT}}$ method³⁹.

RNA interference and bioassays. To synthesize dsRNA, a 529 bp fragment of *CYP6ER1* and a 688 bp fragment of *GFP* [GenBank: ACY56286] were amplified via PCR using the *N.lugens* cDNA as a template. PCR primers are listed in Table S1. The dsRNA synthesis step was performed as described previously³⁷. For the RNAi efficiency evaluation, 0.05, 0.1 and 0.2 micrograms of ds*CYP6ER1* were injected into the side of the abdomen of synchronous one-day-old female *N.lugens* macropterous using a 10 µl micro-syringe (Hamilton). The control injection was performed with an equivalent volume of ds*GFP*. Each experimental group had 30 individuals. Ten adults were selected randomly at 24 h, 36 h and 48 h after injection for the independent detection of *CYP6ER1*. Total RNA extraction and qRT-PCR detection were performed as described above. For the susceptibility detection after RNAi, thirty adults from each group were chosen 24 h after injection, with 0.05 micrograms of ddH₂O, ds*GFP* and ds*CYP6ER1* for each one day-old macropterous female adult. Thirty adults were placed in rice soaked in a solution of 240 ng/µl imidacloprid for 30 seconds. The *N.lugens* mortality was calculated after 96 hours. Each experiment was repeated in triplicate.

Developmental expression and tissue distribution analysis. The expression of *CYP6ER1* were estimated by qRT-PCR as described³⁸ from the first instar nymphs to 13-day-old female adults from the field-caught strain without imidacloprid. To investigate the expression of *CYP6ER1* in different tissues, we extracted the total RNA from the fat body, ovary, midgut, muscle, Malpighian tubule and cuticle. The following steps were performed as described³⁸.

Construction of Transgenic *Drosophila* and Bioassays. The *CYP6ER1* CDS cloned was inserted into a pValium20 vector to prepare UAS-*CYP6ER1* constructs. Subsequently, the constructs were microinjected into the embryos of the γ sc v nanos-integrase; attP2 *D. melanogaster* germline using standard techniques in the Center of Biomedical Analysis, Tsinghua University. The transformed line was crossed with an Act5C-GAL4 line for expression of the *CYP6ER1* gene. The genotype of the cross was Act5C > *CYP6ER1*. For use as a control, the transformed line and the Act5C-GAL4 line were crossed with the W¹¹¹⁸ line, the progenies of which did not express *CYP6ER1* gene with the genotype of UAS-*CYP6ER1* and Act5C-GAL4. RT-PCR was used to confirm the expression of the *CYP6ER1* gene in transgenic *Drosophila* using primers specific for the *CYP6ER1* gene and the reference housekeeping gene *DmActin*⁴⁰. For each cross, total RNA was extracted from 10 adults using the methods described above and three biological replicates were performed for each experiment. The reaction conditions were 94 °C for 5 min, 30 cycles of 94 °C for 30 s, 58 °C for 30 s, and 72 °C for 30 s, using GoTaq G2 Green Master Mix (Promega). Twenty 1–3 day old adults (10 females and 10 males) were used in the contact bioassays, as described previously⁴¹. In brief, flies were placed in vials with 10 ml corn meal medium containing 300 µg imidacloprid. Three replicates were performed for each assay. After 72 h, the survival rates were calculated and analyzed using the Chi-squared test.

Homology modelling. The structure of *CYP6ER1* was predicted using the Homology Modeling protocol of Discovery Studio 2.5. A BLAST search against the PDB_nr95 database was used to search the homology sequence by using the E-value 10–10 as a parameter. A multi sequence alignment between *CYP6ER1* and homology sequences was performed to obtain the best reference for the homology model building. An ideal homologous model should cover as much of the Alignment Length of our target sequence as possible, while keeping relatively high Positive and Sequence identity, which was also analyzed via Align Multiple Sequence in Discovery Studio with default parameters. The crystal structure of human CYP3A4 with the highest resolution and good stereochemistry was used to build the homology model. The best model for subsequent optimization was chosen according to the total PDF energy, PDF physical energy and DOPE score, using Cut overhangs, refine loops and the use DOPE method as parameters.

Molecular dynamics simulations. According to the covalent bonds between ritonavir (RIT) and CYP3A4, we speculated that bonding also occurred between imidacloprid (IM4) and *CYP6ER1*, though conventional docking programs cannot be utilized to generate the ligand-bound conformations. Observing charge distribution in local structures of imidacloprid and *CYP6ER1* calculated by the Gaussian-09 program at the HF/6-31G* level (Gaussian 09, revision a.02. Gaussian Inc., Wallingford)⁴², we found 4, 5-dihydro-1H-imidazole in structural imidacloprid was partly similar to the thiazole structures of RIT. Therefore, it is possible that nitrogen atoms in the heterocycle of the imidachloprid molecule bonded to iron atoms via 4, 5-dihydro-1H-imidazole. A comparison of the electrostatic distributions of RIT and IM4 suggests that IM4 likely has the same binding mode as RIT, and IM4 was found to be manually docked into CYPYER1. A molecular dynamics (MD)-based optimization assessment of the complex structure of CYPYER1 protein was performed with the Discovery Studio 2.5 Dynamics (Heating or Cooling, Equilibration and Production) Module under the CHARMM force field⁴³. The partial charge and implicit solvent model were set to Momany-Rone and generalized born as the molecular dynamics (MD)-based optimization parameters, Electrostatics as Spherical cutoff, Apply SHAKE constraint as True, Minimization as 400, Heating as 2,000, Equilibration as 2,000, Production as 100,000 and other parameters as the defaults.

References

1. Matsumura, M. & Sanada-Morimura, S. Recent Status of Insecticide Resistance in Asian Rice Planthoppers. *Jarq-Jpn Agr Res Q* **44**, 225–230 (2010).
2. Georghiou, G. P. & Mellon, R. B. In Pest Resistance to Pesticides. (eds. Georghiou, G.P. & Saito, T.) 1–46 (Springer US, Boston, MA; 1983).
3. Nagata, T. Monitoring on Insecticide Resistance of the Brown Planthopper and the White Backed Planthopper in Asia. *Journal of Asia-Pacific Entomology* **5**, 103–111 (2002).
4. Davies, T. G., Field, L. M., Usherwood, P. N. & Williamson, M. S. DDT, pyrethrins, pyrethroids and insect sodium channels. *IUBMB Life* **59**, 151–162 (2007).

5. Kimura, Y. Resistance to Malathion in the Small Brown Planthopper, *Laodelphax striatellus* FALLÉN. *Japanese Journal of Applied Entomology & Zoology* **9**, 251–258 (1965).
6. Zibae, A., Sendi, J. J., Ghadamyari, M., Alinia, F. & Etebari, K. Diazinon resistance in different selected strains of *Chilo suppressalis* (Lepidoptera: Crambidae) in northern Iran. *J Econ Entomol* **102**, 1189–1196 (2009).
7. Dai, S. M. & Sun, C. N. Pyrethroid Resistance and Synergism in *Nilaparvata lugens* Stål (Homoptera: Delphacidae) in Taiwan. *Journal of Economic Entomology* **77**, 891–897 (1984).
8. Su, J. Y. *et al.* Status of Insecticide Resistance of the Whitebacked Planthopper, *Sogatella furcifera* (Hemiptera: Delphacidae). *Fla Entomol* **96**, 948–956 (2013).
9. Gorman, K., Liu, Z., Denholm, I., Bruggen, K. U. & Nauen, R. Neonicotinoid resistance in rice brown planthopper, *Nilaparvata lugens*. *Pest Management Science* **64**, 1122–1125 (2008).
10. Zhao, X. *et al.* Differential resistance and cross-resistance to three phenylpyrazole insecticides in the planthopper *Nilaparvata lugens* (Hemiptera: Delphacidae). *J Econ Entomol* **104**, 1364–1368 (2011).
11. Gorman, K. *et al.* Cross-resistance relationships between neonicotinoids and pymetrozine in *Bemisia tabaci* (Hemiptera: Aleyrodidae). *Pest Management Science* **66**, 1186–1190 (2010).
12. Feyereisen, R. Insect P450 enzymes. *Annu Rev Entomol* **44**, 507–533 (1999).
13. Farnham, A. W. The Mode of Action of Piperonyl Butoxide with Reference to Studying Pesticide Resistance - Piperonyl Butoxide - 12. *Piperonyl Butoxide*, 199–213 (1999).
14. Daborn, P. J. *et al.* A single p450 allele associated with insecticide resistance in *Drosophila*. *Science* **297**, 2253–2256 (2002).
15. Liu, N. & Scott, J. G. Increased transcription of CYP6D1 causes cytochrome P450-mediated insecticide resistance in house fly. *Insect Biochem Mol Biol* **28**, 531–535 (1998).
16. Terhzaz, S. *et al.* A novel role of *Drosophila* cytochrome P450-4e3 in permethrin insecticide tolerance. *Insect Biochem Mol Biol* **67**, 38–46 (2015).
17. Crossthwaite, A. J., Rendine, S., Stenta, M. & Slater, R. Target-site resistance to neonicotinoids. *J Chem Biol* **7**, 125–128 (2014).
18. Liu, Z. W. *et al.* Selection for imidacloprid resistance in *Nilaparvata lugens*: cross-resistance patterns and possible mechanisms. *Pest Management Science* **59**, 1355–1359 (2003).
19. Bass, C. *et al.* Overexpression of a cytochrome P450 monooxygenase, CYP6ER1, is associated with resistance to imidacloprid in the brown planthopper, *Nilaparvata lugens*. *Insect Mol Biol* **20**, 763–773 (2011).
20. Bao, H. B. *et al.* The roles of CYP6AY1 and CYP6ER1 in imidacloprid resistance in the brown planthopper: Expression levels and detoxification efficiency. *Pestic Biochem Phys* **129**, 70–74 (2016).
21. Chiu, T. L., Wen, Z., Rupasinghe, S. G. & Schuler, M. A. Comparative molecular modeling of *Anopheles gambiae* CYP6Z1, a mosquito P450 capable of metabolizing DDT. *Proc Natl Acad Sci USA* **105**, 8855–8860 (2008).
22. Lertkitmongkol, P., Jenwitheesuk, E. & Rongnoparut, P. Homology modeling of mosquito cytochrome P450 enzymes involved in pyrethroid metabolism: insights into differences in substrate selectivity. *BMC Research Notes* **4**, 1–7 (2011).
23. Baudry, J., Rupasinghe, S. & Schuler, M. A. Class-dependent sequence alignment strategy improves the structural and functional modeling of P450s. *Protein Eng Des Sel* **19**, 345–353 (2006).
24. de Graaf, C., Vermeulen, N. P. E. & Feenstra, K. A. Cytochrome P450 in silico: An integrative modeling approach. *J Med Chem* **48**, 2725–2755 (2005).
25. Jones, R. T. *et al.* Homology modelling of *Drosophila* cytochrome P450 enzymes associated with insecticide resistance. *Pest Management Science* **66**, 1106–1115 (2010).
26. Karunker, I. *et al.* Structural model and functional characterization of the *Bemisia tabaci* CYP6CM1vQ, a cytochrome P450 associated with high levels of imidacloprid resistance. *Insect Biochem Molec* **39**, 697–706 (2009).
27. Li, X., Schuler, M. A. & Berenbaum, M. R. Molecular mechanisms of metabolic resistance to synthetic and natural xenobiotics. *Annu Rev Entomol* **52**, 231–253 (2007).
28. Rauch, N. & Nauen, R. Identification of biochemical markers linked to neonicotinoid cross resistance in *Bemisia tabaci* (Hemiptera: Aleyrodidae). *Arch Insect Biochem* **54**, 165–176 (2003).
29. Puinean, A. M., Denholm, I., Millar, N. S., Nauen, R. & Williamson, M. S. Characterisation of imidacloprid resistance mechanisms in the brown planthopper, *Nilaparvata lugens* Stal (Hemiptera: Delphacidae). *Pestic Biochem Phys* **97**, 129–132 (2010).
30. Philippou, D., Field, L. & Moores, G. Metabolic enzyme(s) confer imidacloprid resistance in a clone of *Myzus persicae* (Sulzer) (Hemiptera: Aphididae) from Greece. *Pest Management Science* **66**, 390–395 (2010).
31. Le Goff, G. *et al.* Xenobiotic response in *Drosophila melanogaster*: sex dependence of P450 and GST gene induction. *Insect Biochem Mol Biol* **36**, 674–682 (2006).
32. Puinean, A. M. *et al.* Amplification of a Cytochrome P450 Gene Is Associated with Resistance to Neonicotinoid Insecticides in the Aphid *Myzus persicae*. *Plos Genet* **6** (2010).
33. Lesca, P., Rafidinarivo, E., Lecoite, P. & Mansuy, D. A class of strong inhibitors of microsomal monooxygenases: The elupticines. *Chemico-Biological Interactions* **24**, 189–197 (1979).
34. Hedley, D., Khambay, B. P. S., Hooper, A. M., Thomas, R. D. & Devonshire, A. L. Proinsecticides effective against insecticide-resistant peach-potato aphid (*Myzus persicae* (Sulzer)). *Pesticide Science* **53**, 201–208 (1998).
35. Graham, S. E. & Peterson, J. A. How similar are P450s and what can their differences teach us? *Arch Biochem Biophys* **369**, 24–29 (1999).
36. Jousen, N., Heckel, D. G., Haas, M., Schuphan, I. & Schmidt, B. Metabolism of imidacloprid and DDT by P450 GYP6G1 expressed in cell cultures of *Nicotiana tabacum* suggests detoxification of these insecticides in CYP6G1-overexpressing strains of *Drosophila melanogaster*, leading to resistance. *Pest Management Science* **64**, 65–73 (2008).
37. Pang, R. *et al.* Identification of promoter polymorphisms in the cytochrome P450 CYP6AY1 linked with insecticide resistance in the brown planthopper, *Nilaparvata lugens*. *Insect Mol Biol* **23**, 768–778 (2014).
38. Chen, J. *et al.* Feeding-based RNA interference of a trehalose phosphate synthase gene in the brown planthopper, *Nilaparvata lugens*. *Insect Mol Biol* **19**, 777–786 (2010).
39. Livak, K. J. & Schmittgen, T. D. Analysis of relative gene expression data using real-time quantitative PCR and the 2(T)(-Delta Delta C) method. *Methods* **25**, 402–408 (2001).
40. Ponton, F., Chapuis, M. P., Pernice, M., Sword, G. A. & Simpson, S. J. Evaluation of potential reference genes for reverse transcription-qPCR studies of physiological responses in *Drosophila melanogaster*. *J Insect Physiol* **57**, 840–850 (2011).
41. Daborn, P., Boundy, S., Yen, J., Pittendrigh, B. & French-Constant, R. DDT resistance in *Drosophila* correlates with Cyp6g1 overexpression and confers cross-resistance to the neonicotinoid imidacloprid. *Mol Genet Genomics* **266**, 556–563 (2001).
42. Caricato, M., Trucks, G. W. & Frisch, M. J. On the difference between the transition properties calculated with linear response- and equation of motion-CCSD approaches. *J Chem Phys* **131** (2009).
43. Brooks, B. R. *et al.* CHARMM: The Biomolecular Simulation Program. *J Comput Chem* **30**, 1545–1614 (2009).

Acknowledgements

We thank Abhishek Ojha (School of Life Sciences, Sun Yat-sen University, Guangzhou, China) for his comments on the manuscript. This work was funded by the National Natural Science Foundation of China (U1401212) and the Science and Technology Planning Project of Guangdong Province, China (2016A050502021).

Author Contributions

W.Z. designed the conception and reviewed the manuscript. R.P. and M.C. performed the research and wrote the paper. R.P., M.C., Z.L. and H.G. analyzed the data. X.Y. provided *Drosophila* and constructed transgenic *Drosophila*.

Additional Information

Supplementary information accompanies this paper at <http://www.nature.com/srep>

Competing financial interests: The authors declare no competing financial interests.

How to cite this article: Pang, R. *et al.* Functional analysis of *CYP6ER1*, a P450 gene associated with imidacloprid resistance in *Nilaparvata lugens*. *Sci. Rep.* **6**, 34992; doi: 10.1038/srep34992 (2016).



This work is licensed under a Creative Commons Attribution 4.0 International License. The images or other third party material in this article are included in the article's Creative Commons license, unless indicated otherwise in the credit line; if the material is not included under the Creative Commons license, users will need to obtain permission from the license holder to reproduce the material. To view a copy of this license, visit <http://creativecommons.org/licenses/by/4.0/>

© The Author(s) 2016